Predicting and Tracking Short Term Disease Progression in Amnestic Mild Cognitive Impairment Patients with Prodromal Alzheimer's Disease: Structural Brain Biomarkers

Moira Marizzoni[a,*], Clarissa Ferrari[b], Jorge Jovicich[c], Diego Albani[d], Claudio Babiloni[e,f],
Libera Cavaliere[a], Mira Didic[g,h], Gianluigi Forloni[d], Samantha Galluzzi[a], Karl-Titus Hoffmann[i],
José Luis Molinuevo[j], Flavio Nobili[k], Lucilla Parnetti[l], Pierre Payoux[m], Federica Ribaldi[a,n],
Paolo Maria Rossini[o], Peter Schönknecht[p], Marco Salvatore[q], Andrea Soricelli[q], Tilman Hensch[p],
Magda Tsolaki[r], Pieter Jelle Visser[s], Jens Wiltfang[t,u,v], Jill C. Richardson[w], Régis Bordet[x],
Olivier Blin[y], Giovanni B. Frisoni[a,z] and The PharmaCog Consortium

[a]*Laboratory of Neuroimaging and Alzheimer's Epidemiology, IRCCS Istituto Centro San Giovanni di Dio Fatebenefratelli, Brescia, Italy*
[b]*Unit of Statistics, IRCCS Istituto Centro San Giovanni di Dio Fatebenefratelli, Brescia, Italy*
[c]*Center for Mind/Brain Sciences, University of Trento, Italy*
[d]*Neuroscience Department, IRCCS - Istituto di Ricerche Farmacologiche Mario Negri, Milano, Italy*
[e]*Department of Physiology and Pharmacology "V. Erspamer", Sapienza University of Rome, Rome, Italy*
[f]*IRCCS San Raffaele Pisana of Rome, Rome, Italy*
[g]*Aix-Marseille Université, Inserm, INS UMR_S 1106, Marseille, France*
[h]*APHM, Timone, Service de Neurologie et Neuropsychologie, APHM Hôpital Timone Adultes, Marseille, France*
[i]*Department of Neuroradiology, University of Leipzig, Leipzig, Germany*
[j]*Alzheimer's Disease Unit and Other Cognitive Disorders Unit, Hospital Clínic de Barcelona, and Institut d'Investigacions Biomédiques August Pi i Sunyer (IDIBAPS), Barcelona, Catalunya, Spain*
[k]*Clinical Neurology, Dept. of Neuroscience (DINOGMI), University of Genoa and IRCCS AOU San Martino-IST, Genoa, Italy*
[l]*Clinica Neurologica, Università di Perugia, Ospedale Santa Maria della Misericordia, Perugia, Italy*
[m]*INSERM; Imagerie cérébrale et handicaps neurologiques UMR 825, Toulouse, France*
[n]*Department of Molecular and Translational Medicine, University of Brescia, Brescia, Italy*
[o]*Area of Neuroscience, Department of Gerontology, Neurosciences & Orthopedics, Catholic University, Policlinic A. Gemelli Foundation Rome, Italy*
[p]*Department of Psychiatry and Psychotherapy, University of Leipzig, Leipzig, Germany, Germany*
[q]*SDN Istituto di Ricerca Diagnostica e Nucleare, Napoli, Italy*

---

*Correspondence to: Moira Marizzoni, Laboratory of Neuroimaging and Alzheimer's Epidemiology, IRCCS Istituto Centro San Giovanni di Dio Fatebenefratelli, via Pilastroni 4, 25125 - Brescia, Italy. Tel.: +39 030 3501362; Fax: +39 030 3501592; E-mail: mmarizzoni@fatebenefratelli.eu.

r3rd Neurologic Clinic, Medical School, G. Papanikolaou Hospital, Aristotle University of Thessaloniki, Thessaloniki, Greece

sDepartment of Neurology, Alzheimer Centre, VU Medical Centre, Amsterdam, The Netherlands

tLVR-Hospital Essen, Department of Psychiatry and Psychotherapy, Faculty of Medicine, University of Duisburg-Essen, Essen, Germany

uDepartment of Psychiatry and Psychotherapy, University Medical Center (UMG), Georg-August-University, Goettingen, Germany

viBiMED, Medical Sciences Department, University of Aveiro, Aveiro, Portugal

wNeurosciences Therapeutic Area, GlaxoSmithKline R&D, Gunnels Wood Road, Stevenage, United Kingdom

xUniversity of Lille, Inserm, CHU Lille, U1171 - Degenerative and vascular cognitive disorders, Lille, France

yAix Marseille University, UMR-CNRS 7289, Service de Pharmacologie Clinique, AP-HM, Marseille, France

zMemory Clinic and LANVIE - Laboratory of Neuroimaging of Aging, University Hospitals and University of Geneva, Geneva, Switzerland

Abstract.

Background: Early Alzheimer's disease (AD) detection using cerebrospinal fluid (CSF) biomarkers has been recommended as enrichment strategy for trials involving mild cognitive impairment (MCI) patients.

Objective: To model a prodromal AD trial for identifying MRI structural biomarkers to improve subject selection and to be used as surrogate outcomes of disease progression.

Methods: APOE $\varepsilon4$ specific CSF $A\beta_{42}$/P-tau cut-offs were used to identify MCI with prodromal AD ($A\beta_{42}$/P-tau positive) in the WP5-PharmaCog (E-ADNI) cohort. Linear mixed models were performed 1) with baseline structural biomarker, time, and biomarker × time interaction as factors to predict longitudinal changes in ADAS-cog13, 2) with $A\beta_{42}$/P-tau status, time, and $A\beta_{42}$/P-tau status × time interaction as factors to explain the longitudinal changes in MRI measures, and 3) to compute sample size estimation for a trial implemented with the selected biomarkers.

Results: Only baseline lateral ventricle volume was able to identify a subgroup of prodromal AD patients who declined faster (interaction, $p = 0.003$). Lateral ventricle volume and medial temporal lobe measures were the biomarkers most sensitive to disease progression (interaction, $p \leq 0.042$). Enrichment through ventricular volume reduced the sample size that a clinical trial would require from 13 to 76%, depending on structural outcome variable. The biomarker needing the lowest sample size was the hippocampal subfield GC-ML-DG (granule cells of molecular layer of the dentate gyrus) ($n = 82$ per arm to demonstrate a 20% atrophy reduction).

Conclusion: MRI structural biomarkers can enrich prodromal AD with fast progressors and significantly decrease group size in clinical trials of disease modifying drugs.

Keywords: Alzheimer's disease, biomarkers, clinical trial, magnetic resonance imaging, mild cognitive impairment, precision medicine

INTRODUCTION

Clinical trials of Alzheimer's disease (AD) modifiers have invariably failed in the past 15 years [1–3]. Failures have often been attributed to slow disease progression in the placebo group, thus greatly reducing the chance to detect a drug effect in the treated group. Moreover, the standard outcome used to assess global cognition in AD clinical trials so far, is the Alzheimer's Disease Assessment Scale-Cognitive (ADAS-Cog) [4], quite insensitive to mild progression in the early AD stages [5, 6].

Neurodegeneration detected on magnetic resonance imaging (MRI) is known to be a valuable support for cohort enrichment [7–10] and to be more sensitive to change than cognitive outcomes [11]. Structural MRI alterations similar to those found in AD patients have been reported also in mild cognitive impairment (MCI) patients [12–19]. However, to the best of our knowledge, a systematic analysis on imaging features that predict progression and their relationship with AD pathological cerebrospinal fluid (CSF) biomarkers in the MCI stage does not exist.

We studied a group of slowly progressing prodromal AD patients and have examined a wide range

of structural biomarkers to select the best ones to improve prodromal AD trial design 1) by increasing the homogeneity of the eligible population and 2) by identifying reliable outcomes of disease progression. Prodromal AD patients were selected based on APOE-specific CSF $A\beta_{42}$/P-tau cut-offs [35]. First, we assessed the baseline structural biomarkers for their ability in selecting patients who declined faster within the $A\beta_{42}$/P-tau positive group. At the same time, we longitudinally compared global and regional neurodegeneration and white matter microstructural alterations between $A\beta_{42}$/P-tau positive and negative aMCI patients in order to select biomarkers of short term disease progression. Finally, we evaluated the effect of the selected biomarkers on sample size estimation.

MATERIALS AND METHODS

Study population

Data used in this study were obtained from the European ADNI (E-ADNI) database, developed in workpackage 5 (WP5) of IMI PharmaCog project (Innovative Medicine Initiative, http://www.imi.europa.eu/content/pharma-cog) and stored on the neuGRID platform (https://neugrid4you.eu/). Between December 2011 and June 2013, 147 amnestic mild cognitive impairment (aMCI) patients were enrolled in 13 European memory clinics (see Galluzzi et al. [20] for the complete list). Follow-up examinations were performed every 6 months for 2 years or until patient progressed to clinical dementia (follow-up was 20 ± 8 months, minimum: 6 months). Inclusion and exclusion criteria have been described in detail elsewhere [20]. Briefly, the main inclusion criteria were age between 55 and 90 years; complaints of memory loss by the patient or family relative, and confirmed by family relative; Mini-Mental State Examination (MMSE) [21] score of 24 and higher; overall Clinical Dementia Rating [22] score of 0.5; score on the logical memory test [23] lower than 1 standard deviation from the age-adjusted mean, 15-item Geriatric Depression Scale [24] score of 5 or lower, and absence of significant other neurologic, systemic or psychiatric illness.

MRI processing

All MRI scans were performed on 3.0 Tesla machines. MRI protocols were harmonized and pipelines were optimized and described in detail elsewhere [25–27]. Briefly, within-session T1 averaging was performed and all structural images were processed using the longitudinal pipeline of FreeSurfer v6.0 to automatically generate subject-specific cortical thickness and subcortical volume [28–32]. The segmentation results were visually inspected prior to the volume and thickness analyses to confirm that no major errors had occurred. No manual editing was performed. All FreeSurfer analyses were performed on the neuGRID platform (https://neugrid4you.eu/). Diffusion tensor imaging (DTI) scans were preprocessed using DTIPrep tool for automatic quality assurance, which included motion and Eddy current correction for all subjects [33]. The corrected data were then processed using FSL for skull and nonbrain tissue removal (BET) and to extract diffusion maps. White matter (WM) regions-of-interest (ROIs) are predefined in the Johns Hopkins University-ICBM-FA-1 mm atlas and were backprojected with a nonlinear co-registration to each subject's diffusion maps on trackbased spatial statistics (TBSS) space [34]. The analysis was focused on ROI which are of relevance in MCI studies (Supplementary Table 1). Left and right measures were averaged for each subject.
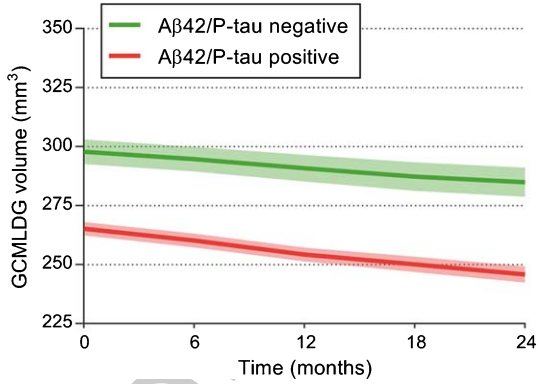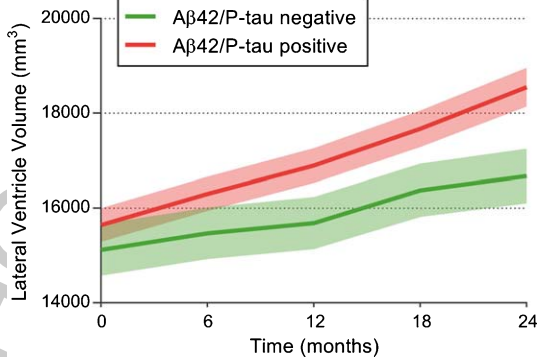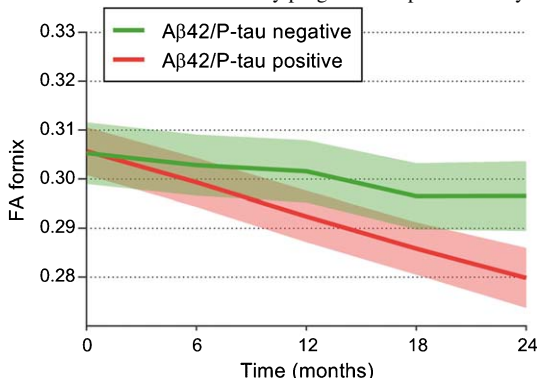
Patients classification

Patients were dichotomized into $A\beta_{42}$/P-tau positive or negative based on baseline CSF $A\beta_{42}$/P-tau level as well as APOE genotype. In particular, $A\beta_{42}$/P-tau positivity was defined as ratio lower than 15.2 for APOE $\varepsilon 4$ carriers and 8.9 for non-carriers as revealed by the mixture model analysis earlier performed [35]. CSF and blood analysis have been performed at the selected central site and described elsewhere [20]. Briefly, $A\beta_{42}$, total tau (T-tau), and P-tau were quantified in the CSF by ELISA kits (Innogenetics, Belgium) according to the manufacturer's instructions. Blood DNA was used for APOE genotyping in a real-time polymerase chain reaction (PCR) using dedicated TaqMan probes (Life Technologies, Carlsbad, CA, USA).

Statistical analysis

Statistical analyses were performed using SPSS for descriptive statistics and R: A language and environment for statistical computing (version 3.4.1) [36]. Baseline participants characteristics were assessed by parametric t-test (or corresponding non-parametric Mann-Whitney) for continuous Gaussian (or

Table 1
Model interpretation and exemplary MRI structural biomarkers selected based on LMM-2 results

LMM-2 outcome (Significant factors, $p < 0.05$)	Model interpretation
Time × Aβ_{42}/P-tau status Time Aβ_{42}/P-tau status	Aβ_{42}/P-tau positive and negative patients show biomarker differences already at baseline. The biomarker progressed faster in positives compared to negatives.

Time × Aβ_{42}/P-tau status Time	Aβ_{42}/P-tau positive and negative patients did not show biomarker differences at baseline. The biomarker progressed faster in positives compared to negatives.

Time × Aβ_{42}/P-tau status	Aβ_{42}/P-tau positive and negative patients did not show biomarker differences at baseline. The biomarker slowly progressed in positives only.

FA, fractional anisotropy; GC-ML-DG, granule cells in the molecular layer of the dentate gyrus.

non-Gaussian) distributed variables and by Chi-square test for categorical data.

Two different types of Linear Mixed Models (LMMs, performed by R-package lme4) were applied with all available timepoints in Aβ_{42}/P-tau positive patients only, to evaluate their sensitivity in picking-up different cognitive trajectories (LMMs-1), and in the whole MCI cohort, to select structural

measures that progressed faster in $A\beta_{42}$/P-tau positive compared to negative patients (LMMs-2). Random intercept and random slope were considered to account for individual differences at baseline as well as for individual change over follow-up (see details in Supplementary Methods 1). The output of the LMMs were presented in terms of standardized β coefficient, corresponding *p*-value and, for the interaction factor only, effect size (pseudo η^2) calculated as the ratio of explained variability of interaction effect on total variability of each model.

LMMs-1 were conducted with baseline biomarker measures, time and biomarker × time interaction as covariates to predict cognitive decline measured as longitudinal changes in ADAS-cog13 score. For this model, volumes and thicknesses were obtained from the cross-sectional processing of the baseline T1 scans. Only $A\beta_{42}$/P-tau positive patients were included. All models were adjusted for age, sex and education. The distribution of the biomarker showing the smallest *p*-value for the "biomarker × time interaction" factor was tested for the presence of components and cut-offs able to distinguish any subgroups. To this purpose, the mclust and flexmix packages of R were applied in order to perform finite mixture model [37, 38]. The estimation procedure was carried out by Expectation-Maximization algorithm [39], whereas the number of components and the parametrization of each of them (i.e., the 'best-fit' model) was chosen by the Bayesian Information Criterion (BIC) indexes: lower indexes values indicate best model [40]. The cut-off for distinguishing components was defined as the biomarker value for which the mixture model assigned equal probability of belonging to two consecutive components.

LMMs-2 were conducted with time, group (corresponding to CSF status), time × group interaction as covariates. All models were further adjusted for age, sex and baseline MMSE and volumes LMMs also for total intracranial volume (TIV). Only biomarkers with significant group × time interaction were reported, meaning that they differently progressed over-time between groups (for detailed on model interpretation refers to Table 1).

Finally, the effect of biomarkers-based enrichment and end-points was assessed in the design of a 2-year clinical trial of disease modifiers applying a sample size calculation for linear mixed models with baseline covariates [41]. Sample size was calculated for a 20 and 30% reduction of biomarker slope by fixing a significant level for type I error equal to 0.05 and a power of 0.8 for a two-sided test.

RESULTS

CSF quantification and APOE genotype were available for 144 out of 147 aMCI patients of Pharmacog/E-ADNI. The characteristics of these subjects classified according to their baseline $A\beta_{42}$/P-tau ratio value as well as APOE genotype are shown in Table 2. $A\beta_{42}$/P-tau positive MCI patients were similar for age, gender, and education compared to negative patients but showed worse global cognitive performance as measured using MMSE ($p = 0.006$) and higher CSF T-tau levels ($p < 0.001$).

Biomarkers sensitive to cognitive decline

Global cognition slightly improved in the $A\beta_{42}$/P-tau negative patients and declined in the positive group as indicated by a decrease and an increase of the ADAS-cog13 score, respectively (time × CSF status interaction effect, $p < 0.001$) (Fig. 1A). As in prodromal AD trials only prodromal AD patients are included, we evaluated the sensitivity of each baseline structural biomarker to predict different ADAS-cog13 trajectories within the $A\beta_{42}$/P-tau positive group (LMMs-1). The analysis of the proportion of variability in ADAScog13 score over time explained by time, baseline biomarker values and time × biomarker interaction reported a significant interaction only for the lateral ventricle volume (time × biomarker interaction, $p = 0.003$, standardized $\beta = 0.287$, $\eta^2 = 0.29$). This means that high or low values of the lateral ventricle volume were able to predict different longitudinal ADAS-cog13 trajectories.

Mixture model was applied on the baseline lateral ventricle volume (LVV) distribution of $A\beta_{42}$/P-tau positive MCI patients to test for the existence of subgroups. The analysis reported the presence of 2 subgroups (BIC for 2 component-model = 1645 compared to BIC = 1659 for the 1 component-model and BIC = 1658 for the 3 component-model) and one cut-off value of 14330 mm^3 (Supplementary Figure 1). Patients with large LVV (>14330 mm^3) were older ($p = 0.006$), mainly males ($p = 0.006$), had higher education ($p = 0.024$) and showed worse MMSE score ($p = 0.024$) compared to patients with small LVV (<14330 mm^3) (Table 3). According to LMM1 results, subjects with large LVV declined more rapidly on the ADAS-cog13 compared to those with small LVV (Fig. 1B).

Table 2
Clinical and socio-demographic features of aMCI patients stratified into $A\beta_{42}$/P-tau positive and negative according to APOE4-specific cut-offs

	$A\beta_{42}$/P-tau negative $(n=63)$	$A\beta_{42}$/P-tau positive $(n=81)$	p^a
Age, mean (SD)	68.3 (8.4)	69.8 (6.3)	0.208
Sex, F/M, No.	36/27	46/35	1.000
Education, mean (SD)	10.0 (4.3)	11.1 (4.4)	0.115
APOE $\varepsilon4$ carriers, No. (%)	3 (5)	63 (78)	**<0.001**
MMSE, mean (SD)	27.1 (1.8)	26.2 (1.8)	**0.006**
ADAS-cog13, mean (SD)^{b,c}	19.1 (5.9)	21.6 (8.1)	0.052
CSF biomarkers, mean (SD, pg/ml)			
$A\beta_{42}$	949 (244)	495 (132)	**<0.001**
P-Tau	47 (15)	84 (38)	**<0.001**
T-tau	301 (149)	614 (394)	**<0.001**

^{a}Assessed by ANOVA (for continuous Gaussian distributed variables) or Kruskall-Wallis with Dunn correction (for continuous non-Gaussian distributed variables) and Chi-square tests (for categorical variables). ^{b}Range 0–85, with 0 as the best score. ^{c}Information was missing for 1 patient. Values significant at the 5% level are bold. ADAS-cog13, Alzheimer Disease Assessment Scale-Cognitive Subscale, version 13; $A\beta_{42}$, amyloid-β; APOE, apolipoprotein E; CSF, cerebrospinal fluid; MMSE, Mini-Mental State Examination; P-tau, tau phosphorylated at threonine 181; T-tau, total tau.
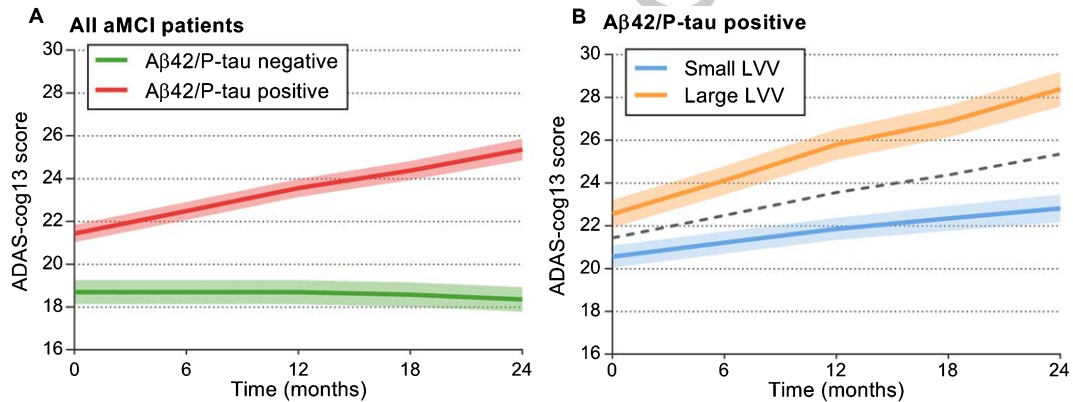

Fig. 1. Longitudinal ADAS-cog13 changes (A) in $A\beta_{42}$/P-Tau positive and negative MCI patients and (B) in the $A\beta_{42}$/P-Tau positive MCI patients stratified according to LVV classification. Graphs illustrate the estimated values and 95% confidence intervals obtained from the respective linear mixed models. Dotted line in (B) refers to ADAScog13 estimated values in the $A\beta_{42}$/P-Tau positive group. ADAScog13 range was 0–85, with higher score indicating worst performance. The ventricular volume cut-off was established by mixture model analysis (Supplementary Figure 1).

Surrogate outcome of disease progression

Next, we examined the ability of each biomarker in separating positive and negative aMCI patients to identify those that progressed faster in the positive group. Table 4 shows the proportion of variability in MRI measures over time explained by time, $A\beta_{42}$/P-tau status and time × $A\beta_{42}$/P-tau status interaction (LMMs-2) for the biomarkers reporting a significant effect of the interaction. Volumes of lateral ventricle, hippocampus and several its subfields, amygdala as well as entorhinal thickness showed the strongest association with disease progression in MCI with prodromal AD (time × $A\beta_{42}$/P-tau status inter-

action, $p < 0.042$, $-0.101 < $ std $\beta < -0.032$, $0.06 < \eta^2 < 0.24$). This means that the longitudinal course of the structural measures is different in $A\beta_{42}$/P-tau positive and negative MCI groups. For example, the model regarding the lateral ventricle volume estimated that $A\beta_{42}$/P-tau positive had an expansion of the volume 0.077 times higher than negative patients every six months and thus, 0.308 times higher in 2 years. Conversely, a reduction of the GC-ML-DG (granule cells of molecular layer of the dentate gyrus) volume was 6-monthly estimated 0.068 time higher (0.272 time in 2 years) in positive compared to negative patients. Of note, medial temporal lobe (MTL) regions were atrophic already at baseline in $A\beta_{42}$/P-tau positive

Table 3
Clinical and socio-demographic features of $A\beta_{42}$/P-tau positive MCI patients stratified
according to lateral ventricle volume (LVV)

	Small LVV ($n = 45$)	Large LVV ($n = 36$)	p^a
Age, mean (SD)	68.1 (5.9)	71.9 (6.2)	**0.006**
Females, No. (%)	32 (71)	14 (39)	**0.006**
Education, mean (SD)	10.1 (4.0)	12.3 (4.6)	**0.024**
APOE ε4 carriers, No. (%)	33 (73)	30 (83)	0.420
MMSE, mean (SD)	26.6 (1.9)	25.7 (1.7)	**0.024**
ADAS-cog13, mean (SD)[b,c]	20.2 (6.6)	23.3 (9.5)	0.091
CSF biomarkers, mean (SD, pg/ml)			
$A\beta_{42}$	505 (139)	481 (123)	0.655
P-Tau	90 (43)	76 (29)	0.151
T-tau	669 (475)	545 (247)	0.398

[a] Assessed by ANOVA (for continuous Gaussian distributed variables) or Kruskall-Wallis with Dunn correction (for continuous non-Gaussian distributed variables) and Chi-square tests (for categorical variables). [b] Range 0–85, with 0 as the best score. [c] Information was missing for 1 patient. Values significant at the 5% level are bold. ADAS-cog13, Alzheimer Disease Assessment Scale-Cognitive Subscale, version 13; $A\beta_{42}$, amyloid-β; APOE, apolipoprotein E; CSF, cerebrospinal fluid; LVV, lateral ventricle volume; MMSE, Mini-Mental State Examination; P-tau, tau phosphorylated at threonine 181; T-tau, total tau.

compared with negative MCI patients ($A\beta_{42}$/P-tau status, $p < 0.004$, $-0.418 <$ std $\beta < -0.248$). Among microstructural indexes, only fractional anisotropy (FA) in the fornix showed a different longitudinal alteration in MCI groups (time $\times$ $A\beta_{42}$/P-tau status interaction, $p = 0.007$, std $\beta = 0.137$, $\eta^2 = 0.09$).

Surrogate outcomes for disease modifiers

The selected biomarkers of short term disease progression (listed in Table 4) were compared with ADAS-cog13 in terms of sample size required to observe a 20 and 30% treatment effect and power of 0.8 (Table 5). Within the $A\beta_{42}$/P-tau MCI positive group, to observe a 20% of treatment effect, meaning a slope reduction of 20%, the ADAS-cog13 score required 662 subjects per arm. Volumes were those requiring the lower number of subjects and the hippocampal volume was the best, needing 116 subjects. Besides hippocampal volume, excellent performance was found for two of its subfields, the GC-ML-DG with 123 subjects and the molecular layer with 131 subjects.

Further gain in power was reached with almost all biomarkers by selecting the $A\beta_{42}$/P-tau MCI positive with large LVV. Exception were: CA3 and fimbria, which lost power; lateral ventricle, cerebral WM and istmus cingulate remained unaltered. Again, to observe a reduction of 20% in slope, the biomarker needing the lowest number of subjects is the hippocampal subfield GC-ML-DG, 82, followed by CA4, 83, and the hippocampal volume calculated as sum of each subfield, 84.

DISCUSSION

In the PharmaCog/E-ADNI study, designed as a clinical trial in the aMCI population, we examined a wide range of structural and microstructural biomarkers known to be altered in MCI patients. The goal was to select the best ones to improve prodromal AD trial design 1) by increasing the homogeneity of the eligible population and 2) by identifying reliable outcomes of disease progression. Thus, we evaluated the effect of the selected biomarkers in a 2-year clinical trial involving $A\beta_{42}$/P-tau positive MCI patients with a target of 20 or 30% slowing of disease atrophy treatment effect and power of 0.8. Importantly, we did not include the MCI population as a whole in our sample size calculation or in the enrichment analysis as MCI patient selection based on AD pathological biomarkers is the general practice in prodromal AD trial.

Consistently with recent evidence [8, 9, 42], we found that the assessment of neurodegeneration on MRI increased the statistical power of clinical trials by reducing the sample size required when using CSF cut-offs alone. Indeed, further selection of $A\beta_{42}$/P-tau positive MCI patients by using the baseline LVV classification reduced the sample size that a clinical trial would require from 13 to 76%, depending on the outcome considered. Moreover, we confirmed the greater power of MRI measures to detect longitudi-

Table 4
Ability of MRI structural biomarkers to separate CSF $A\beta_{42}$/P-tau Positive and Negative aMCI patients

Measure	Time X $A\beta_{42}$/P-tau status			Time		$A\beta_{42}$/P-tau status	
	Std β	p	Effect size	Std β	p	Std β	p
Lateral Ventricle	0.077	**<0.001**	0.48	0.063	**<0.001**	0.112	0.216
GC-ML-DG	–0.068	**<0.001**	0.24	–0.073	**<0.001**	–0.289	**<0.001**
Molecular layer HP	–0.064	**<0.001**	0.24	–0.069	**<0.001**	–0.315	**<0.001**
CA4	–0.065	**<0.001**	0.22	–0.068	**<0.001**	–0.301	**<0.001**
Whole HP (subfields sum)	–0.060	**<0.001**	0.21	–0.065	**<0.001**	–0.336	**<0.001**
Entorhinal	–0.101	**0.001**	0.21	–0.043	**0.010**	–0.248	**0.004**
HP	–0.069	**<0.001**	0.20	–0.083	**<0.001**	–0.307	**<0.001**
Subiculum	–0.061	**<0.001**	0.18	–0.046	**<0.001**	–0.323	**<0.001**
Presubiculum	–0.064	**0.001**	0.17	–0.048	**<0.001**	–0.281	**<0.001**
CA3	–0.050	**0.004**	0.14	–0.059	**<0.001**	–0.270	**<0.001**
Hippocampal tail	–0.048	**0.006**	0.11	–0.064	**<0.001**	–0.418	**<0.001**
Isthmus cingulate	–0.073	**0.016**	0.10	–0.042	**0.012**	–0.068	0.400
Temporal pole	–0.065	**0.010**	0.09	–0.045	**0.001**	–0.076	0.400
Amygdala	–0.048	**0.007**	0.09	–0.047	**<0.001**	–0.275	**<0.001**
FA fornix	–0.137	**0.007**	0.09	–0.024	0.393	–0.118	0.153
Fimbria volume	–0.070	**0.043**	0.08	–0.035	0.070	–0.147	0.055
Parahippocampal	–0.059	**0.039**	0.07	–0.016	0.316	–0.133	0.135
CA1	–0.032	**0.042**	0.06	–0.059	**<0.001**	–0.259	**<0.001**
Cerebral WM	–0.038	**0.040**	0.05	–0.078	**<0.001**	–0.093	0.138
CC Mid Anterior	–0.141	**0.045**	0.05	0.026	0.497	–0.088	0.303

Linear mixed models for volume analyses included age, sex, baseline MMSE, TIV, time, $A\beta_{42}$/P-tau status, time × $A\beta_{42}$/P-tau status interaction as predictors. Linear mixed models for thickness and DTI parameter analyses included age, sex, baseline MMSE, time, $A\beta_{42}$/P-tau status, time × $A\beta_{42}$/P-tau status interaction as predictors. Only biomarkers with significant Time × $A\beta_{42}$/P-tau status interaction effect ($p < 0.05$) are shown. Values significant at the 5% level are bold. CA, Cornu Ammonis; CC, corpus callosum; FA, fractional anisotropy; GC-ML-DG, Granule cells in the molecular layer of the dentate gyrus; HP, hippocampus; Std, Standardized; WM, white matter.

nal changes compared to ADAScog13 [11, 43–45]. The presented results show that hippocampus is the region most sensitive to disease progression and confirms its feasibility to be used as surrogate outcome for a clinical trial of disease modifiers in MCI with prodromal AD. In $A\beta_{42}$/P-tau positive MCI patients considered as a whole, the most significant gain of power was obtained by using the hippocampal volume. When combined enrichment was applied, the biomarkers needing the smallest sample size was the hippocampal subfield GC-ML-DG that would require 82 subjects compared to ADAScog13 and hippocampal volume needing 364 and 87 subjects, respectively.

Compared to previous reports focused on multi-biomarker enrichment, we applied a data driven approach to select the best biomarker for cohort enrichment. Among all the biomarkers found altered in the MCI stage we investigated, the linear mixed model showed that only LVV was sensitive in picking up different ADAScog13 trajectories within the $A\beta_{42}$/P-tau positive MCI patients. We expected to find a similar association between baseline hippocampal volume, to date the only qualified biomarker for enrichment of clinical trials in pre-dementia stages of AD [10], and ADAScog13 progression but, surprisingly, we did not. Previous

findings demonstrated that baseline LVV examination improved risk prediction in MCI patients [46] and reduced sample size in AD clinical trials better than MTL measures [47–49]. Moreover, a stronger correlation with changes on cognitive tests was reported for LVV enlargement compared with hippocampal atrophy rates [48]. In patients with MCI, this association has previously been observed in APOE ε4 carriers only [43] who were overrepresented in the prodromal AD group of the present study. The higher sensitivity of LVV compared to MTL regions in predicting different cognitive decline within the $A\beta_{42}$/P-tau positive MCI patients may be related to methodological and biological issues. Hence, considering that a large portion of the ventricle is adjacent to MTL regions, LVV likely reflects the AD-related atrophy that occur in this region in the pre-clinical stages of dementia [50, 51] and, conversely to hippocampus, measurement is more robust and less prone to segmentation errors giving the sharp contrast between the signal intensity of CSF in the ventricles and surrounding tissue in T1-weighted MRI images. Furthermore, LVV may also reflects atrophy in other regions than the MTL and likely represents a global measure of neurodegeneration as whole-brain volume, which correlates with clinical progression

Table 5
Sample size estimates required in each arm of a placebo-controlled trial in $A\beta_{42}$/P-tau positive
MCI patients to observe 20% and 30% atrophy reduction of brain structural outcomes

| | $A\beta42$/P-tau positive (n/arm) | | | | Sample size reduction |
| | All | | With large LVV | | |
	20%	30%	20%	30%	%
ADAS-Cog13	662	294	364	162	–45
Lateral Ventricle	193	86	182	81	–6
GC-ML-DG	123	55	**82**	**36**	–33
Molecular layer HP	131	58	90	40	–31
CA4	133	59	83	37	–37
Whole HP (subfields sum)	141	63	84	37	–41
Entorhinal	407	181	285	126	–30
HP	**116**	**52**	87	39	–25
Subiculum	237	105	196	87	–17
Presubiculum	266	118	135	60	–49
CA3	227	101	259	115	14
Hippocampal tail	236	105	162	72	–31
Isthmus cingulate	544	242	553	247	2
Temporal pole	508	226	324	144	–36
Amygdala	364	162	87	39	–76
FA fornix	749	333	497	221	–13
Fimbria volume	1077	479	1941	863	80
Parahippocampal	1446	643	400	178	–72
CA1	269	120	170	76	–37
Cerebral WM	168	75	164	73	–2
CC Mid Anterior	6769	3009	1742	774	–74

Sample size calculations are based on linear mixed models performed in all $A\beta_{42}$/P-Tau positive patients and in those with large baseline lateral ventricle volume assuming a 20, 30% slope reduction of the outcome in a 2-year trial with scans every six months. All calculations were performed by fixing significant level of type I error of 0.05, power equal to 0.8 and not controlling for normal aging. The ventricular volume cut-off was established by mixture model analysis (Supplementary Figure 1). ADAS-cog13, Alzheimer Disease Assessment Scale-Cognitive Subscale, version 13; CA, Cornu Ammonis; FA, fractional anisotropy; GC-ML-DG, Granule cells in the molecular layer of the dentate gyrus; HP, hippocampus; LVV, lateral ventricle volume; WM, white matter.

[48, 52, 53]. A more intriguing and less investigated scenario considers ventricular dilation as a marker of altered CSF dynamics and a biological proxy for faulty CSF clearance mechanisms in AD [54]. Failure of the CSF to clear potentially toxic metabolites would lead to accumulation of $A\beta_{42}$, P-tau, and perhaps other toxins in the brain and thus, may have a role in the onset and progression of AD [55, 56]. This would give a plausible biological explanation on the reason why aMCI patients with prodromal AD and with large LVV showed faster cognitive decline compared to those with small LVV. Moreover, it suggests that, when the CSF AD biomarkers are present at pathological levels, LVV may be a valuable biomarker to distinguish fast and slow decliners.

Our 2-year longitudinal analysis reported the strongest association between baseline CSF pathological values and progressive deterioration in key AD regions such as hippocampus, several of its subfields and entorhinal cortex. Although these structural abnormalities have been extensively reported in aMCI and AD patients, to the best of our knowledge,

no one has investigated their longitudinal changes in aMCI patients as a function of CSF pathology. Besides grey matter atrophy, prodromal AD patients exhibited also a slightly progressive WM degeneration as indicated by WM shrinkage at global level and in the middle/anterior portion of the corpus callosum. Moreover, MRI diffusion revealed a progressive structural connectivity reduction in the fornix, important for episodic memory recall [57], which is in line with progressive involvement of the posterior mesiotemporal network in prodromal AD [58], especially as a change in FA of the fornix did not differ in $A\beta_{42}$/P-tau positive and negative patients at baseline, but progressed slowly in positives only.

Demonstration of disease-modifying therapies efficacy is garnered through clinical trial designs and biomarkers [59]. Enhanced disease understanding can be translated into better clinical trial design by increasing the chance to enroll individuals who have a higher probability to positively respond to drugs (and reducing the adverse events) and by identifying those markers most likely to be sensitive to

pharmacological manipulation. Moreover, in the AD field, where no effective treatment is available at the moment, selective enrolment applying CSF Aβ_{42} and P-tau biomarkers as well as APOE genotype can be applied for testing innovative treatments targeting not only amyloid but also tangles or APOE-related phenomena.

The main limitation of the study is the lack of a healthy control group. We did not consider the effect of structural changes due to normal aging in our sample size calculation. Similarly, we did not account for other important variables impacting the efficiency of clinical trials, such as participants drop out or screening failure rates. Thus, a real trial would likely involve a larger number of participants than reported in the present study. Secondly, the study is limited by the absence of the validation in an independent population, but the purpose here was to investigate a typical clinical trial population. We provided initial evidence of the benefit that LVV based enrichment could have. However, further investigations to confirm the LVV sensitivity in identifying fast decliners in MCI with prodromal AD are needed.

In conclusion, the selection of homogeneous aMCI patients using a multi-biomarker strategy enables to test the efficacy of new drugs in prodromal AD trial in relatively small groups of mildly progressing patients. Baseline lateral ventricular volume was the best biomarker to be used for cohort enrichment and volume of the GC-ML-DG hippocampal subfield was the ideal outcome measure when considering trials of MCI population enriched for CSF AD biomarker.

DISCLOSURE STATEMENT

Authors' disclosures available online (https://www.j-alz.com/manuscript-disclosures/18-0152r2).

SUPPLEMENTARY MATERIAL

The supplementary material is available in the electronic version of this article: http://dx.doi.org/10.3233/JAD-180152.

REFERENCES

[1] Fleisher AS (2010) NerveCenter: Phase III Alzheimer trial halted: Search for therapeutic biomarkers continues. *Ann Neurol* **68**, A9-A12.

[2] Green RC, Schneider LS, Amato DA, Beelen AP, Wilcock G, Swabb EA, Zavitz KH, Tarenflurbil Phase 3 Study Group (2009) Effect of tarenflurbil on cognitive decline and activities of daily living in patients with mild Alzheimer disease: A randomized controlled trial. *JAMA* **302**, 2557-2564.

[3] Vellas B, Carrillo MC, Sampaio C, Brashear HR, Siemers E, Hampel H, Schneider LS, Weiner M, Doody R, Khachaturian Z, Cedarbaum J, Grundman M, Broich K, Giacobini E, Dubois B, Sperling R, Wilcock GK, Fox N, Scheltens P, Touchon J, Hendrix S, Andrieu S, Aisen P (2013) Designing drug trials for Alzheimer's disease: What we have learned from the release of the phase III antibody trials: A report from the EU/US/ CTAD Task Force. *Alzheimers Dement* **9**, 438-444.

[4] Rosen WG, Mohs RC, Davis KL (1984) A new rating scale for Alzheimer's disease. *Am J Psychiatry* **141**, 1356-1364.

[5] Samtani MN, Raghavan N, Shi Y, Novak G, Farnum M, Lobanov V, Schultz T, Yang E, Dibernardo A, Narayan VA (2013) Disease progression model in subjects with mild cognitive impairment from the Alzheimer's disease neuroimaging initiative: CSF biomarkers predict population subtypes. *Br J Clin Pharmacol* **75**, 146-161.

[6] Brooks LG, Loewenstein DA (2010) Assessing the progression of mild cognitive impairment to Alzheimer's disease: Current trends and future directions. *Alzheimers Res Ther* **2**, 28.

[7] Grill JD, Di L, Lu PH, Lee C, Ringman J, Apostolova LG, Chow N, Kohannim O, Cummings JL, Thompson PM, Elashoff D (2013) Estimating sample sizes for predementia Alzheimer's trials based on the Alzheimer's Disease Neuroimaging Initiative. *Neurobiol Aging* **34**, 62-72.

[8] Holland D, McEvoy LK, Desikan RS, Dale AM; Alzheimer's Disease Neuroimaging Initiative (2012) Enrichment and stratification for predementia Alzheimer disease clinical trials. *PLoS One* **7**, e47739.

[9] Wolz R, Schwarz AJ, Gray KR, Yu P, Hill DLG (2016) Enrichment of clinical trials in MCI due to AD using markers of amyloid and neurodegeneration. *Neurology* **87**, 1235-1241.

[10] Hill DLG, Schwarz AJ, Isaac M, Pani L, Vamvakas S, Hemmings R, Carrillo MC, Yu P, Sun J, Beckett L, Boccardi M, Brewer J, Brumfield M, Cantillon M, Cole PE, Fox N, Frisoni GB, Jack C, Kelleher T, Luo F, Novak G, Maguire P, Meibach R, Patterson P, Bain L, Sampaio C, Raunig D, Soares H, Suhy J, Wang H, Wolz R, Stephenson D (2014) Coalition Against Major Diseases/European Medicines Agency biomarker qualification of hippocampal volume for enrichment of clinical trials in predementia stages of Alzheimer's disease. *Alzheimers Dement* **10**, 421-429.

[11] Schuff N, Woerner N, Boreta L, Kornfield T, Shaw LM, Trojanowski JQ, Thompson PM, Jack CR, Weiner MW (2009) MRI of hippocampal volume loss in early Alzheimers disease in relation to ApoE genotype and biomarkers. *Brain* **132**, 1067-1077.

[12] Clerx L, van Rossum IA, Burns L, Knol DL, Scheltens P, Verhey F, Aalten P, Lapuerta P, Van de Pol L, Van Schijndel R, De Jong R, Barkhof F, Wolz R, Rueckert D, Bocchetta M, Tsolaki M, Nobili F, Wahlund LO, Minthon L, Frölich L, Hampel H, Soininen H, Visser PJ (2013) Measurements of medial temporal lobe atrophy for prediction of Alzheimer's disease in subjects with mild cognitive impairment. *Neurobiol Aging* **34**, 2003-2013.

[13] Leung KK, Bartlett JW, Barnes J, Manning EN, Ourselin S, Fox NC (2013) Cerebral atrophy in mild cognitive impairment and Alzheimer disease: Rates and acceleration. *Neurology* **80**, 648-654.

[14] Tabatabaei-Jafari H, Shaw ME, Cherbuin N (2015) Cerebral atrophy in mild cognitive impairment: A systematic review with meta-analysis. *Alzheimers Dement (Amst)* **1**, 487-504.

[15] Gutiérrez-Galve L, Lehmann M, Hobbs NZ, Clarkson MJ, Ridgway GR, Crutch S, Ourselin S, Schott JM, Fox NC, Barnes J (2009) Patterns of cortical thickness according to APOE genotype in alzheimer's disease. *Dement Geriatr Cogn Disord* **28**, 476-485.

[16] Dickerson BC, Wolk DA (2013) Biomarker-based prediction of progression in MCI: Comparison of AD signature and hippocampal volume with spinal fluid amyloid-β and tau. *Front Aging Neurosci* **5**, 55.

[17] Elahi S, Bachman AH, Lee SH, Sidtis JJ, Ardekani BA (2015) Corpus callosum atrophy rate in mild cognitive impairment and prodromal Alzheimer's disease. *J Alzheimers Dis* **45**, 921-931.

[18] Lee SH, Bachman AH, Yu D, Lim J, Ardekani BA (2016) Predicting progression from mild cognitive impairment to Alzheimer's disease using longitudinal callosal atrophy. *Alzheimers Dement (Amst)* **2**, 68-74.

[19] Bai F, Zhang Z, Watson DR, Yu H, Shi Y, Yuan Y, Qian Y, Jia J (2009) Abnormal integrity of association fiber tracts in amnestic mild cognitive impairment. *J Neurol Sci* **278**, 102-106.

[20] Galluzzi S, Marizzoni M, Babiloni C, Albani D, Antelmi L, Bagnoli C, Bartres-Faz D, Cordone S, Didic M, Farotti L, Fiedler U, Forloni G, Girtler N, Hensch T, Jovicich J, Leeuwis A, Marra C, Molinuevo JL, Nobili F, Pariente J, Parnetti L, Payoux P, Del Percio C, Ranjeva JP, Rolandi E, Rossini PM, Schönknecht P, Soricelli A, Tsolaki M, Visser PJ, Wiltfang J, Richardson JC, Bordet R, Blin O, Frisoni GB (2016) Clinical and biomarker profiling of prodromal Alzheimer's disease in workpackage 5 of the Innovative Medicines Initiative PharmaCog project: A "European ADNI study." *J Intern Med* **279**, 576-591.

[21] Folstein MF, Folstein SE, McHugh PR (1975) Mini-Mental State: A practice method for grading the cognitive state of patients for the clinician. *J Psychiatr Res* **12**, 189-198.

[22] Morris JC (1993) The Clinical Dementia Rating (CDR): Current version and scoring rules. *Neurology* **43**, 2412-2414.

[23] Woodard JL, Axelrod BN (1987) Wechsler memory scale - revised. *Psychol Assess* **7**, 445-449.

[24] Brown LM, Schinka JA (2005) Development of initial validation of a 15-item informant version of the Geriatric Depression Scale. *Int J Geriatr Psychiatry* **20**, 911-918.

[25] Jovich J1, Marizzoni M, Sala-Llonch R, Bosch B, Bartrés-Faz D, Arnold J, Benninghoff J, Wiltfang J, Roccatagliata L, Nobili F, Hensch T, Tränkner A, Schönknecht P, Leroy M, Lopes R, Bordet R, Chanoine V, Ranjeva JP, Didic M, Gros-Dagnac H, Payoux P, Zoccatelli G, Alessandrini F, Beltramello A, Bargalló N, Blin O, Frisoni GB; PharmaCog Consortium (2013) Brain morphometry reproducibility in multi-center 3T MRI studies: A comparison of cross-sectional and longitudinal segmentations. *Neuroimage* **83**, 472-484.

[26] Marizzoni M, Antelmi L, Bosch B, Bartrés-Faz D, Müller BW, Wiltfang J, Fiedler U, Roccatagliata L, Picco A, Nobili F, Blin O, Bombois S, Lopes R, Sein J, Ranjeva JP, Didic M, Gros-Dagnac H, Payoux P, Zoccatelli G, Alessandrini F, Beltramello A, Bargalló N, Ferretti A, Caulo M, Aiello M, Cavaliere C, Soricelli A, Salvadori N, Parnetti L, Tarducci R, Floridi P, Tsolaki M, Constantinidis M, Drevelegas A, Rossini PM, Marra C, Hoffmann KT, Hensch T, Schönknecht P, Kuijer JP, Visser PJ, Barkhof F, Bordet R,

Frisoni GB, Jovicich J (2015) Longitudinal reproducibility of automatically segmented hippocampal subfields: A multisite European 3T study on healthy elderly. *Hum Brain Mapp* **36**, 3516-3527.

[27] Jovicich J, Marizzoni M, Bosch B, Bartres-Faz D, Arnold J, Benninghoff J, Wiltfang J, Roccatagliata L, Picco A, Nobili F, Blin O, Bombois S, Lopes R, Bordet R, Chanoine V, Ranjeva J-P, Didic M, Gros-Dagnac H, Payoux P, Zoccatelli G, Alessandrini F, Beltramello A, Bargallo N, Ferretti A, Caulo M, Aiello M, Ragucci M, Soricelli A, Salvadori N, Tarducci R, Floridi P, Tsolaki M, Constantinidis M, Drevelegas A, Rossini PM, Marra C, Otto J, Reiss-Zimmermann M, Hoffmann K-T, Galluzzi S, Frisoni GB (2014) Multi-site longitudinal reliability of tract-based spatial statistics in diffusion tensor imaging of healthy elderly subjects. *Neuroimage* **101**, 390-403.

[28] Dale AM, Fischl B, Sereno MI (1999) Cortical surface-based analysis: I. Segmentation and surface reconstruction. *Neuroimage* **9**, 179-194.

[29] Fischl B, Van Der Kouwe A, Destrieux C, Halgren E, Ségonne F, Salat DH, Busa E, Seidman LJ, Goldstein J, Kennedy D, Caviness V, Makris N, Rosen B, Dale AM (2004) Automatically parcellating the human cerebral cortex. *Cereb Cortex* **14**, 11-22.

[30] Fischl B, Salat DH, Busa E, Albert M, Dieterich M, Haselgrove C, Van Der Kouwe A, Killiany R, Kennedy D, Klaveness S, Montillo A, Makris N, Rosen B, Dale AM (2002) Whole brain segmentation: Automated labeling of neuroanatomical structures in the human brain. *Neuron* **33**, 341-355.

[31] Reuter M, Schmansky NJ, Rosas HD, Fischl B (2012) Within-subject template estimation for unbiased longitudinal image analysis. *Neuroimage* **61**, 1402-1418.

[32] Iglesias JE, Augustinack JC, Nguyen K, Player CM, Player A, Wright M, Roy N, Frosch MP, McKee AC, Wald LL, Fischl B, Van Leemput K (2015) A computational atlas of the hippocampal formation using ex vivo, ultra-high resolution MRI: Application to adaptive segmentation of *in vivo* MRI. *Neuroimage* **115**, 117-137.

[33] Oguz I, Farzinfar M, Matsui J, Budin F, Liu Z, Gerig G, Johnson HJ, Styner M (2014) DTIPrep: Quality control of diffusion-weighted images. *Front Neuroinform* **8**, 4.

[34] Smith SM, Jenkinson M, Johansen-Berg H (2006) Tract-based spatial statistics: Voxelwise analysis of multi-subject diffusion data. *Neuroimage* **31**, 1487-1505.

[35] Marizzoni M, Ferrari C, Galluzzi S, Jovicich J, Albani D, Babiloni C, Didic M, Forloni G, Molinuevo JL, Nobili FM, Parnetti L, Payoux P, Rossini PM, Schönknecht P, Soricelli A, Tsolaki M, Visser PJ, Wiltfang J, Bordet R, Cavaliere L, Richardson J, Blin O, Frisoni GB (2018) CSF biomarkers and effect of apolipoprotein E genotype, age and sex on cut-off derivation in mild cognitive impairment. *Alzheimers Dement* **13**, P1319.

[36] R Developement Core Team (2015) R: A language and environment for statistical computing. *R Found Stat Comput* **1**, 409.

[37] McLachlan G, Peel D (2000) *Finite Mixture Models*, John Wiley and Sons, New York.

[38] Fraley C, Raftery, Adrian E (2007) Model-based methods of classification: Using the mclust software in chemometrics. *J Stat Softw* **18**, 1-13.

[39] Dempster AP, Laird NM, Rubin DB (1977) Maximum likelihood from incomplete data via the EM algorithm. *J R Stat Soc Ser B Methodol* **39**, 1-38.

[40] Burnham KP, Anderson DR, Huyvaert KP (2011) AIC model selection and multimodel inference in behavioral ecology: Some background, observations, and comparisons. *Behav Ecol Sociobiol* **65**, 23-35.

[41] Liu G, Liang K-Y (1997) Sample size calculations for studies with correlated observations. *Biometrics* **53**, 937.

[42] Holland D, McEvoy LK, Dale AM (2012) Unbiased comparison of sample size estimates from longitudinal structural measures in ADNI. *Hum Brain Mapp* **33**, 2586-2602.

[43] Nestor SM, Rupsingh R, Borrie M, Smith M, Accomazzi V, Wells JL, Fogarty J, Bartha R (2008) Ventricular enlargement as a possible measure of Alzheimer's disease progression validated using the Alzheimer's disease neuroimaging initiative database. *Brain* **131**, 2443-2454.

[44] Fujishima M, Kawaguchi A, Maikusa N, Kuwano R, Iwatsubo T, Matsuda H (2017) Sample size estimation for Alzheimer's disease trials from Japanese ADNI serial magnetic resonance imaging. *J Alzheimers Dis* **56**, 75-88.

[45] Holland D, Brewer JB, Hagler DJ, Fennema-Notestine C, Dale AM (2009) Subregional neuroanatomical change as a biomarker for Alzheimer's disease. *Proc Natl Acad Sci U S A* **106**, 20954-20959.

[46] McEvoy LK, Holland D, Hagler DJ, Fennema-Notestine C, Brewer JB, Dale AM (2011) Mild cognitive impairment: Baseline and longitudinal structural MR imaging measures improve predictive prognosis. *Radiology* **259**, 834-843.

[47] Fox NC, Cousens S, Scahill R, Harvey RJ, Rossor MN (2000) Using serial registered brain magnetic resonance imaging to measure disease progression in Alzheimer disease - Power calculations and estimates of sample size to detect treatment effects. *Arch Neurol* **57**, 339-344.

[48] Jack CR, Shiung MM, Gunter JL, O'Brien PC, Weigand SD, Knopman DS, Boeve BF, Ivnik RJ, Smith GE, Cha RH, Tangalos EG, Petersen RC, Petersen RC (2004) Comparison of different MRI brain atrophy rate measures with clinical disease progression in AD. *Neurology* **62**, 591-600.

[49] Schott JM, Price SL, Frost C, Whitwell JL, Rossor MN, Fox NC (2005) Measuring atrophy in Alzheimer disease: A serial MRI study over 6 and 12 months. *Neurology* **65**, 119-124.

[50] Ferrarini L, Palm WM, Olofsen H, van Buchem MA, Reiber JHC, Admiraal-Behloul F (2006) Shape differences of the brain ventricles in Alzheimer's disease. *Neuroimage* **32**, 1060-1069.

[51] Giesel FL, Hahn HK, Thomann PA, Widjaja E, Wignall E, Von Tengg-Kobligk H, Pantel J, Griffiths PD, Peitgen HO, Schroder J, Essig M (2006) Temporal horn index and volume of medial temporal lobe atrophy using a new semi-automated method for rapid and precise assessment. *Am J Neuroradiol* **27**, 1454-1458.

[52] Mungas D, Harvey D, Reed BR, Jagust WJ, DeCarli C, Beckett L, Mack WJ, Kramer JH, Weiner MW, Schuff N, Chui HC (2005) Longitudinal volumetric MRI change and rate of cognitive decline. *Neurology* **65**, 565-571.

[53] Fox NC, Black RS, Gilman S, Rossor MN, Griffith SG, Jenkins L, Koller M (2005) Effects of Abeta immunization (AN1792) on MRI measures of cerebral volume in Alzheimer disease. *Neurology* **64**, 1563-1572.

[54] Ott BR, Cohen R a, Gongvatana A, Okonkwo OC, Johanson CE, Stopa EG, Donahue JE, Silverberg GD, Alzheimer's Disease Neuroimaging Initiative (2010) Brain ventricular volume and cerebrospinal fluid biomarkers of Alzheimer's disease. *J Alzheimers Dis* **20**, 647-657.

[55] Silverberg GD, Mayo M, Saul T, Rubenstein E, McGuire D (2003) Alzheimer's disease, normal-pressure hydrocephalus, and senescent changes in CSF circulatory physiology: A hypothesis. *Lancet Neurol* **2**, 506-511.

[56] Rubenstein E (1998) Relationship of senescence of cerebrospinal fluid circulatory system to dementias of the aged. *Lancet* **351**, 283-285.

[57] Tsivilis D, Vann SD, Denby C, Roberts N, Mayes AR, Montaldi D, Aggleton JP (2008) A disproportionate role for the fornix and mammillary bodies in recall versus recognition memory. *Nat Neurosci* **11**, 834-842.

[58] Didic M, Barbeau EJ, Felician O, Tramoni E, Guedj E, Poncet M, Ceccaldi M (2011) Which memory system is impaired first in alzheimer's disease? *J Alzheimers Dis* **27**, 11-22.

[59] Cummings J, Fox N (2017) Defining disease modifying therapy for Alzheimer's disease. *J Prev Alzheimers Dis* **4**, 109-115.